The Cryosphere Discuss., doi:10.5194/tc-2016-292, 2017
Manuscript under review for journal The Cryosphere
Published: 5 January 2017

Use of an Unmanned Aerial Vehicle to assess recent surface elevation change of Storbreen in Norway

W.W. IMMERZEEL[1,*], P.D.A. KRAAIJENBRINK[1], L.M. ANDREASSSEN[2]

[1]Utrecht University, Department of Physical Geography, PO Box 80115, Utrecht, The Netherlands, w.w.immerzeel@uu.nl

[2]Norwegian Water Resources and Energy Directorate, PO Box 5091, Majorstuen, NO-0301 Oslo, Norway

*Corresponding author

The Cryosphere Discuss., doi:10.5194/tc-2016-292, 2017
Manuscript under review for journal The Cryosphere
Published: 5 January 2017

Abstract

Routinely and accurate monitoring of the outlines and surface mass balance of glaciers is essential. In this study an unmanned aerial vehicle (UAV) was used in September 2015 on a mountain glacier (Storbreen) in Norway to map the glacier outline, snow line and to derive a digital elevation model (DEM) of the glacier surface. The generated DEM has a relatively high accuracy with maximum horizontal RMSE of 0.36 m vertical RMSE of 0.44 m and the Structure for Motion algorithm also proved to be suitable under low contrast, high saturation fully snow covered conditions. A well distributed set of markers, measured by GPS, was required to generate a high quality DEM under the yielding conditions. The final UAV DEM was compared to a laser based DEM of 2009 and the annual geodetic mass balance between 2015 and 2009 was estimated to be between -0.71 ± 0.1 m w.e. and -0.75 m ± 0.1 w.e., which is in good agreement with the glaciological mass balance of -0.80 m ± 0.18 w.e. a^{-1}. An analysis of the glacier outlines reveal that the glacier has lost 1.2% of its surface area between 2009 and 2015. These findings confirm the strong mass loss and retreat of continental glaciers in southern Norway.

The Cryosphere Discuss., doi:10.5194/tc-2016-292, 2017
Manuscript under review for journal The Cryosphere
Published: 5 January 2017

1. Introduction

The glaciers in Norway are, as elsewhere in the world, characterized by a reduction in area and a general loss of mass in particular since 2000 (Andreassen et al., 2016; Winsvold et al., 2014).

Climate change is likely to play a major role and understanding the underlying mechanisms are of key importance for both water resources assessments and projections for future sea level rise. There is therefore a great need for systematic and accurate observations with a high spatial detail of glacier mass balances to further advance our understanding of the climate – glacier system.

The surface mass balance of a glacier can be assessed using in-situ point observations (glaciological method) or by repeated surveys using remote sensing (geodetic method). Both methods are independent of each other, yet the differences between them are often substantial (Cogley, 2009) and a homogenisation procedure is required to make a reliable comparison (Zemp et al., 2013). The glaciological method uses point observations of ablation and accumulation (stakes, probings and snow pits), which are spatially interpolated to derive an overall glacier surface mass balance. The geodetic method is based on multi-temporal surveys of surface elevations and can be derived from several sources such as laserscanning (LIDAR), aerial photos or satellite imagery. Surveys can be terrestrial, airborne or from space. The glacier mass balance is quantified by differencing digital elevation models (DEMs) from different years and by converting volume change to mass change using a density conversion. Both the glaciological and geodetic approaches are imperfect as the glaciological method suffers from measurement errors and it is often complicated to measure a sufficiently large number of points on a glacier to derive an accurate interpolated spatial surface mass balance. The geodetic approach often relies on relatively coarse resolution DEMs and significant uncertainties stem from viewing angles, co-registration, density assumption, the glacier areas and masks and inaccurate DEMs in steep terrain (Kääb et al., 2015; Magnússon et al., 2015; Nuth and Kääb, 2011; Pellicciotti et al., 2015; Rolstad et al., 2009). A comparative study for 10 glaciers in Norway with long-term series of glaciological and geodetic mass balance revealed that the discrepancy between the methods was larger than the estimated uncertainty for 7 out of 21 periods studied (Andreassen et al., 2016). The study stresses the need for independent geodetic survey as a way to validate field observations.

Unmanned Aerial Vehicles (UAVs) are not yet commonly used in glaciology, but have a large potential for deriving accurate high resolution DEMs, quantifying surface velocity, thermal mapping and classification of glacier surface features among others (Bhardwaj et al., 2016; Immerzeel et al., 2014; Kraaijenbrink et al., 2016a, 2016b; Ryan et al., 2015; Vincent et al., 2016; Westoby et al., 2016). In the Nepalese Himalayas, for example, a fixed wing UAV was used to derive a pre- and post-monsoon DEM with the aim to investigate the surface lowering and dynamics of a debris covered glacier (Immerzeel et al., 2014). The study showed that it is feasible to derive accurate DEMs at 20 cm resolution for an area of several km^2 with a high accuracy (~25 cm both vertically and horizontally) even in complex terrain. In subsequent studies UAVs were used to automatically derive seasonal flow velocities (Kraaijenbrink et al., 2016a) and to perform an object based classification of supra glacial lakes and ice cliffs (Kraaijenbrink et al., 2016c). The high resolution and accuracy in combination with the on-demand employability potentially provides the opportunity for frequent studies of smaller glaciers.

The software used for generating the UAV based DEMs is based on the structure for motion (SfM) algorithm (Westoby et al., 2012) and it largely relies on automatic matching of features between overlapping images. Therefore, it is likely that DEM generation for snow surfaces and debris free glaciers with limited contrast is challenging and this has not yet been systematically tested. However, recent SfM studies under different conditions (prairies, exposed mountain tops, steep slopes) using different platforms (manned aircraft, copters, fixed wing UAVs) have shown that the accuracy in mapping snow depth in alpine terrain is in the order of 10 cm (Harder et al., 2016; Jagt et al., 2015; De Michele et al., 2016; Nolan et al., 2015). This offers the opportunity to routinely monitory snow and ice surfaces.

In this study, a fixed wing UAV was used in combination with differential Global Navigation Satellite System (dGNNS) measurements on the glacier Storbreen in southern Norway to test whether it is feasible to use the SfM alghoritm to derive an accurate DEM for the snow cover accumulation area and the debris-free ice of the glacier. We compare the UAV results with a LIDAR based DEM from 2009 to quantify spatial changes in the surface mass balance and compare this with the glaciological mass balance data. Finally, we discuss the potential of UAVs in the routinely monitoring of the mass balance of glaciers.

2. Study area

This study focuses on the mountain glacier Storbreen in the Jotunheimen region in southern Norway (Figure 1). Storbreen (61°36' N, 8°8' E) has the longest record of observed mass balance in Norway, measurements started in 1949. Storbreen has been surveyed repeatedly in the past (Andreassen, 1999; Liestøl, 1967) and the latest survey is from 2009 (Andreassen et al., 2016). According to the 2009 survey, Storbreen has an altitude range from 1400 to 2102 m a.s.l. and an average slope of 14° (Andreassen et al., 2016). The glacier has northeastern exposure, Storbreen can be characterized as a short valley or a composite cirque glacier (Liestøl, 1967). The area of the Storbreen has steadily decreased from 7.2 km^2 at the end of the Little Ice Age (~1750) to 6.0 km^2 in 1940 to 5.4 km^2 in 1997 to 5.1 km^2 in 2009 (Andreassen, 1999; Andreassen et al., 2016). Reanalysis of the glaciological and geodetic mass balance series of Storbreen for three periods (1968-1984, 1984-1997 and 1997-2009) showed no statistical difference between the geodetic and glaciological mass balance.

However, the differences were substantial for the 1984-1997 period (Andreassen et al., 2016). Their results show that mass balances for Storbreen have been predominantly negative since 1968, except for a transient mass surplus over 1989-1995 (Andreassen et al., 2005; 2016),

3. Methods and data

3.1. Field surveys

The latest full mapping of the surface elevation of Storbreen was made in 2009 and is used in this study together with the new UAV survey of 2015. In the following, we describe the 2009 and 2015 campaigns.

LIDAR survey 2009

The data from 2009 consist of aerial photos taken on 14 September and airborne LIDAR elevation data of the glacier acquired on 17 October by Blom Geomatics. The time lag for the photography and the laser scanning is due to technical problems with the laser scanner on September 14. Aerial photos were also taken 17 October, but then the glacier was completely snow covered. The surveys were used to produce orthophotos with a 0.4 m resolution and a point elevation cloud with an average point density of about 1.7 points m^{-2}.The glacier outline was digitised manually from the orthophotos from 17 September.

UAV survey 2015

Storbreen was surveyed by an eBee (www.sensefly.com) UAV in 2015 on 9 and 10 September 2015 in fair weather conditions. The UAV was used in six separate flights to cover most of the glacier surface (Fig. 2, Table 2). On September 9 it was launched from the upper part of the glacier and landed nearby on the snow, while on September 10 this was performed at the more easily accessible lower terminus. The UAV was set to take photographs with about 70% overlap. For each flight, the UAV followed waypoints of a predefined flight plan using its built-in GPS. Each waypoint's altitude was determined in the accompanying software by combining a desired ground resolution setting with base elevation data. This helps to achieve a relatively constant UAV altitude with respect to the glacier relief and thus a relatively constant ground resolution. Desired resolutions were set to 6 to 10 cm per pixel, depending on the flight. The camera mounted in the UAV was a 16 megapixel Canon IXUS 127 HS compact camera with customized firmware. The lens was set to its widest setting to reduce the number of required photos and flight time. In total the UAV acquired 915 separate images and covered an area of ~7.5 km^2.

To put the data in a real world coordinate system 31 markers were distributed over accessible parts of Storbreen (Figure 2) before the UAV survey. The markers were made from 1.0 by 0.8 m pieces of garbage bags in black (when positioned on ice or snow on the glacier) or blue (when positioned on debris or rock outcrops on the glacier or rock outside the glacier). To be used as ground control points (GCPs), each marker's approximate centre was measured using a Global Navigation Satellite System (GNSS) rover from Topcon GR3 with an estimated accuracy of 0.1 m in x,y and z.

There were no dedicated independent markers laid out for the determination of the geodetic accuracy of processed UAV data, as the number of markers were thought to be sufficient to leave a few redundant for ground control. For an additional independent indication of the output accuracy, surface profiles of the glacier (Figure 2) were measured using GNSS. This was performed by strapping the GNSS receiver to a backpack and recording its coordinates kinematically at a 1 second interval while traversing the glacier. Antenna height was measured on multiple occasions while standing still, but variation of the antenna height caused by movement of the person was not measured. We estimate the induced error is in the order of 0.3 m. The position of the profile was visually tracked and sampled from the DEM by identifying the xy locations of the footsteps in the snow on the orthomosaic.

Glaciological and meteorological surveys

During the field campaign in September 2015 stake length was measured for the 9 stake locations present on Storbreen and their position was recorded using GNSS. Snow covered most of the glacier and only the lower terminus and some exposed parts were snow free. The depth of the remaining snow was measured at 31 locations on the glacier using a snow probe and the density of the remaining winter snow was measured at three locations (Figure 2). The snow depth data was interpolated to a gridded continuous surface using ordinary kriging.

3.2. UAV data processing

The 915 images from the UAV survey were processed into a 3D model using Structure from Motion (Szelisky, 2011) in the software package Agisoft Photoscan Professional version 1.2.4 (Agisoft LLC, 2014). Several previous studies have used this approach successfully to derive high quality digital elevation models (DEM) (Immerzeel et al., 2014; Kraaijenbrink et al., 2016a; Lucieer et al., 2013; Westoby et al., 2012) . The precise workflow and settings used to process the data are equal to those presented by Kraaijenbrink et al. (2016a, 2016b). To achieve optimal geodetic accuracy of the output product all but one of the markers were used as ground control during processing (Figure 2). One marker was discarded because of an erroneous GNSS measurement, most likely due to poor satellite coverage.

The generated 3D point cloud was post processed in CloudCompare (Lague et al., 2013). The glacier surface was smooth at the time of the survey because of the remaining snow covering most of the glacier. A moderate local outlier filter was therefore applied to remove some erroneous irregularities in the cloud unrelated to the actual relief. The filtered cloud was gridded to a 0.5 m resolution DEM for accuracy assessment. For comparison with the LIDAR dataset from 2009 the point cloud was subsampled to a minimum point distance of 0.5 m. Additionally, the 3D information from the original point cloud was used in Agisoft to generate an orthomosaic, i.e. a stitched raster of orthorectified input images, with a resolution of 0.1 m.

3.3. UAV product accuracy

The geodetic accuracy of the SfM DEM was assessed using two methods: (1) cross-check with the GCP coordinates and (2) comparison with the independent GNSS profile. For the first method, the horizontal errors the difference between the measured marker coordinates and their digitized centres on the orthomosaic were measured. Vertical differences were subsequently quantified by comparing the output DEM elevation with the measured elevation after correcting for the horizontal error. As the GCPs are also used in the SfM DEM generation processes, the differences are a measure of the accuracy of the SfM optimization, whereas the comparison with the GNSS profiles is indicative for the spatial accuracy.

For comparison with the GNSS profile 150 samples were randomly selected from the total of 23,164 points. Candidates were only points that lie further than 100 m from the nearest ground control point and that were recorded while walking steadily. At the points the horizontal error was estimated by measuring the shortest distance perpendicular to the centre of the footprint trail as observed on the orthomosaic, given that the trail was visible at the point under consideration. The difference between the recorded elevation and the DEM elevation at the point was used as indication of vertical error at all points. Horizontal error was here not corrected for, as horizontal errors could not be estimated for all points and as the differences between corrected and uncorrected vertical errors were generally negligible on the smooth glacier surface.

In addition to the geodetic accuracies, local noise in the point cloud was estimated as such noise may affect the accuracy of gridded statistics, e.g. the cloud-derived DEM. The relatively smooth, snow-laden glacier surface was assumed to have little local variation, and high local variation in the point cloud was therefore utilized as noise indicator. To estimate it, linear models were fitted to the subsampled cloud on a 4 by 4 m grid for the entire glacier. The root mean square error (RMSE) of the residuals was then calculated to provide the noise estimate. The off-glacier areas are not smooth and consequently the method was not applied there.

The importance of the number of markers and their distribution on the quality of the generated DEM was evaluated by reprocessing the UAV imagery using 5, 10 and 20 randomly selected markers from the total set of 30 markers. The generated DEMs were compared to the original DEM and the differences were analysed. The analysis was done in those parts of the glacier that are characterized by an RMSE < 0.20 m and which are more than 100 meters away from the glacier margin to avoid undesired effects due to steep slopes.

3.4. Glacier delineation and terminus retreat

A vector outline of the glacier surface was constructed from the orthomosaic using object-based image analysis (Blaschke, 2010). The three-band orthomosaic was resampled to 1 m resolution and used as input for multiresolution segmentation in eCognition Developer 9.1.2 (Trimble, 2015). From the resulting set of polygonal objects a training set of objects with 10 samples for each of the classes ice, snow and other was produced. The training objects were used in a simple fuzzy neighbour classification (Trimble, 2015) as implemented in eCognition Developer. Object characteristics used for classification were the mean and standard deviation of the pixel values present within an object. The glacier outline was corrected by manual digitisation during a visual inspection of the classification, this was needed in particular at the southern tongue which was partly debris covered. In addition, the collected UAV imagery did not cover the entire glacier, some of the uppers parts of Storbreen were missing (Figure 2). To obtain a complete glacier outline, the upper part was replaced by the 2009 outline. Reductions

The Cryosphere Discuss., doi:10.5194/tc-2016-292, 2017
Manuscript under review for journal The Cryosphere
Published: 5 January 2017

in surface area of the glacier and terminus retreat over the past years were determined by comparing the 2015 and 2009 outlines.

3.5. Elevation change

To determine the elevation loss of Storbreen over the period 2009–2015 the post processed UAV point cloud from 2015 was compared with the LIDAR point cloud from 2009. Cloud-to-cloud differences were calculated in CloudCompare using the robust comparison algorithm Multiscale Model to Model Cloud Comparison (Lague et al., 2013), i.e. M3C2. The determined differences were gridded to a 2 m grid for further analysis.

3.6. Geodetic mass balance

Based on the surface elevation change between 17 October 2009 and 9-10 September 2015 a geodetic mass balance was derived. First, the UAV DEM was masked out for areas with a RMSE > 0.2 m (Figure 7) or less than 100 meter from the glacier boundary to avoid any undesired effects due too steep slopes. Based on this mask (Figure 7), the average difference in surface elevation with the LIDAR DEM was computed. The mean elevation change for the area were then corrected for differences in the acquisition date and converted to mass using a density conversion (see results and discussion).

The surface elevation difference was subsequently corrected for fresh snow, which was present in 2009. As a final step the average annual mass balance was computed over the masked area over the 6 year period and an error estimate that includes conservative error estimates for the LIDAR and UAV measurements, snow depth and snow and ice densities.

4. Results and discussion

The ortho-mosaic of the 2015 campaign shows that the glacier was still mostly snow covered and only the lower parts of both tongues and some parts in the ice fall were snow free (fig. 3a). The snow line at the time of the measurements was about 1570 m asl. which has not been so low at the ablation measurements since 1990 (Data: NVE). The snow depth measurements ranged between 0.45 and 1.83 m, with a mean of 1.31 m. Interpolation of the 31 points gave a mean of 0.85 m over the snow covered parts (Figure 7).

As the SfM workflow relies on matching features based on the Scale Invariant Feature Transform (SIFT) in overlapping pictures its application to pristine white snow surfaces could potentially be difficult. However, using the algorithm it was feasible to generate a sufficiently dense spare point cloud to derive a continuous ortho-mosaic and DEM for the entire glacier, including the pristine white upper part of the glacier. This can be attributed to a relatively high height above the surface, e.g. large area coverage per picture and the presence of small scale depressions and surface patterns due to melt and wind erosion on the snow covered glacier picked up by the SIFT algorithm. These findings are in line with previous studies which also do not report any major shortcoming as a result of over saturated pictures or lack of contrast over snow surfaces (Jagt et al., 2015; De Michele et al., 2016; Nolan et al., 2015).

The accuracy of the generated UAV DEM was assessed in four different ways: (i) cross-check with the GCPs, (ii) comparison with the GNSS track over the glacier surface, (iii) comparison with stake observations of 2015 and (iv) assessment of elevation differences between the LIDAR and the UAV DEM outside the glacier. In panel A and B of Figure 4 the horizontal and vertical errors are shown for 30 GCPs. Since these GCPs were used in the processing they cannot be used as an independent validation, however the GCPs give information regarding locational errors resulting from the processing and ortho-rectification. The horizontal GCP RMSE was 0.28 m. and the vertical GCP RMSE was 0.22 m. In panels C and D the horizontal and vertical errors are plotted for independent points which were randomly selected from the DGPS track on the glacier. The horizontal and vertical track RMSEs are 0.36 m. and 0.44 m. respectively, which are slightly higher than for the GCPs. An additional source of error in the latter case is the fact that the antenna was carried in a backpack and its height and horizontal positions may vary while walking. It is also important to note that the vertical errors are well distributed around 0 for both the GCPs and the track and the mean vertical biases are 0.05 and 0.07 m. respectively.

In 2015 the position and surface elevation of the stakes at the glacier surface were also measured using the GNSS one day before and during the same days that the flights were conducted (Figure 2). A comparison between the 2015 data for 10 stakes and the UAV DEM shows that the RMSE is 0.67 m, and if one outlier associated to a GNSS measurement error is omitted the RMSE is 0.41 m.

The elevation difference between the 2009 LIDAR DEM and the 2015 UAV DEM in the off-glacier area was also compared as an independent check (Figure 7). The elevation difference based on the point cloud comparison also takes into account horizontal shifts between the point clouds. The average difference between both DEMs is -0.83 ± 0.78 m for the off-glacier area, suggesting that the 2009 DEM is consistently lower than the 2015 DEM. This is remarkable since the GCPs and track validation do not reveal a systematic bias. A possible explanation may be the presence of snow during the LIDAR campaign in 2009. The LIDAR DEM was acquired on 17 October 2009 and othophotos taken on September 14 and October 17 reveal that a snow layer had built up on the glacier and in the glacier forefield in this period. According to SeNorge, an operational snow model with 1×1 km resolution that uses gridded observations of daily temperature and precipitation as forcing (Saloranta, 2012) the snow depth is 29 cm for the off-glacier area. However, this is only an estimate of the snow depth. Previous studies have shown that seNorge may underestimate the precipitation at Storbreen and cannot describe the local accumulation characteristics in detail (Engelhardt et al, 2012). Temperature data from nearby met station Sognefjellshytta (1413 m. a.s.l.) reveal temperatures below freezing point from 28 September 2009 onwards and precipitation data

The Cryosphere Discuss., doi:10.5194/tc-2016-292, 2017
Manuscript under review for journal The Cryosphere
Published: 5 January 2017

from Bøverdalen (701 m a.s.l.) shows a total of 63 mm of snow between 28 September and 17 October. An average snow depth of 29 cm may therefore be plausible. If accounting for the snow this would still imply a systematic difference of 59 cm between the DEMs outside the glacier. However, the difference may be explained by a larger error in the UAV DEM in the off-glacier area, because there are few GCPs here. In AgiSoft the sparse point cloud is geometrically corrected using the GCPs, however in areas at the margins of the region of interest without GCPs this may cause geometrical artefacts. In the off-glacier area there is indeed larger estimated error, there seems to be a slight north-south gradient in the error and that are areas where the RMSE reach values of 0.5 meter (Figure 7). Hence, the assessment of the off-glacier elevations reveals mostly an artefact of the UAV processing and has no bearing on the on-glacier accuracy.

The experiments where the number of markers used in the AgiSoft processing is varied shows that both the distribution across the glacier and the total number has great bearing on the quality of the generated DEM (Figure 6). The average deviations from the reference DEM where all markers were used are -0.09±0.16 m, 0.02±0.44 m, -0.04±0.11 m for the 5, 10, 20 marker experiments respectively. The 10 marker experiment reveals that the northern and southern parts show relative large deviations. This is caused by the fact that the 10 markers selected are all located on the central part of the glacier. For the 5 marker experiment the markers are more equally distributed across the glaciers and the deviations from the reference DEM is smaller than for the 10 marker experiment, even while the number of markers is halved. The 20 marker experiment shows the best result with only a small average difference and a narrow distribution of the differences. In this case the markers are also relatively well distributed across the glacier surface.

The surface elevation difference map between 2009 and 2015 reveals that the glacier has lowered over the entire surveyed parts in this period. The lower tongue has lowered more than the upper part of the glacier. The lower tongue has lowered between 8 and 10 meters over the 6 years, whereas the upper part of the glacier has lowered between 3 to 6 meters, except for a small area in the northwestern part of the upper glacier, which is an exposed gully of about 20 meter depth and it may be subject to a microclimate, windy conditions and/or a specific radiation budget. The termini of both tongues show the largest elevation change up to 15 meters in the northern terminus to 11 meters on the southern terminus.

The surface elevation changes between October 2009 and September 2015 were used to derive a geodetic mass balance for Storbreen. Only the area within the 2009 extent were used and low accuracy parts (with an UAV RMSE > 0.20 m and more than 100 meter away from the glacier margin to avoid effects of shading and steep slopes) were excluded in the analysis. The total unmasked area is 3.88 km^2 (77% of the total glacier area) (Figure 7). The average elevation change within this area was -5.30 m. To convert the mean elevation difference in meters to a geodetic mass balance in m w.e. and compare with the glaciological mass balance calculated in this period, one must account for ablation and accumulation between the glaciological and the geodetic surveys and make a density conversion (e.g. (Zemp et al., 2013)) The survey for the 2009 DEM was 17 October, a month later than the ablation measurements. The snow cover at this day is part of the 2009/2010 mass balance, and results in a higher surface elevation of the 2009 DEM. In 2015, the UAV survey was at the same time as the ablation measurements. The remaining snow is part of the glaciological mass balance for the mass balance year 2014/2015 and thus the comparison period 2009-2015. However, the remaining snow has a lower density than that of ice. In geodetic calculations, it is a common approach to assume an unchanged density profile from the surface to the firn–ice transition following Sorge's law (Bader, 1954). A density conversion factor of 850±60 kg m^{-3} has been shown to be appropriate for a wide range of conditions (Huss, 2013). However, for shorter periods the density conversion factor can vary significantly.

As mentioned, for the 2009 DEM snow depths we used the SeNorge model simulations giving snow depths of 0.29 m.

Correcting for a mean snow layer of 0.29 m gives a dH of -5.01 m. Assuming Sorges law and applying a density conversion factor of 850 ± 100 kg m^{-3} results in a geodetic mass balance of -4.26±0.60 m w.e. Alternatively, accounting for the lower density of the remaining snow in 2015 gives a slightly more negative balance of -4.47 ± 0.60 m w.e. The mean balance over the six years is then -0.71 ± 0.1 m w.e. and -0.75 m ± 0.1 w.e. respectively.

The cumulative glaciological mass balance over the six balance years from 2009/10 to 2014/2015 is -4.8 m ± 1.1 w.e. or -0.80 m ± 0.18 w.e. a^{-1} (Kjøllmoen et al., 2016).

The new 2015 survey reveal a significant retreat of the terminus since 2009. The southern terminus has retreated around 50 m, whereas the northern termini has retreated about 100 m. NVE's length change measurements, conducted on the southern tongue, show a retreat of 49 m from 2009 to 2014, or 9.8 m/a for the five years. In 2015, the southern terminus was snow covered and the front position was therefore not measured. GNSS survey of the southern terminus on 18 September 2014 (the terminus was snow free when measured) show that the tongue was at nearly the same position in 2014 and 2015, and thus the retreat of the southern tongue occurred from 2009 to 2014, the northern tongue was snow free and likely retreated also in 2015. The total glacier area reduction was 0.06 km^2, a 1.2 % reduction of the 2009 area.

5. Conclusions

In this study a UAV was used on a mountain glacier in Norway to evaluate its potential for mapping and quantifying the surface mass balance. The UAV results were compared to a LIDAR dataset and to the glaciological mass balance and the accuracy of the UAV DEM was assessed using markers and tracks on the glacier, stake measurements and by conducting experiments with varying numbers of markers used in the UAV image processing.

It is concluded that UAVs are an attractive alternative or complementary tool to "traditional" methods such as aerial photography, LIDAR and satellite imagery. The analysis shows that the accuracy of the generated DEM is relatively high and sufficient to quantify the surface mass balance. Key advantages over traditional methods are (i) that the UAV can be used at an optimal time under the best possible weather and light conditions, (ii) that the resolution of the output is very high and (iii) that a DEM and an ortho-mosaic are acquired simultaneously. Disadvantages are that the accuracy may not be high enough for annual campaigns and that the surveys must be accompanied by a number of markers on the surface that requires additional fieldwork. Furthermore, the UAV may not be covering the entire glacier if a suitable launching spot within a horizontal distance of ~2 km and a vertical distance of ~500 meter is unavailable.

The 2015 campaign on Storbreen revealed that the SfM alghoritm also performs well on glacier covered in snow. As long as there are small surface patterns due to wind erosion and melt and the flight altitude is relative large to ensure sufficient variation within a single image, it is feasible to derive an accurate surface DEM also for snow covered surfaces. This provides the opportunity to use UAVs in the annual mapping of glaciers under varying conditions. It is recommended to repeat the campaign under low snow conditions (with a higher transient snow line) to assess whether accuracy of the DEM improves as a result of better contrast and more texture on the glacier surface.

The analysis shows that the use of markers measured by GNSS is essential to derive an accurate ortho-mosaic and DEM from the UAV imagery. The number and the distribution of the markers are important for the accuracy of the final products. It is essential to distribute the markers evenly across the area of interest and to have at least markers at the margins of the

The Cryosphere Discuss., doi:10.5194/tc-2016-292, 2017
Manuscript under review for journal The Cryosphere
Published: 5 January 2017

area of interest. An average of about 6 markers / km^2 equally distributed over the area of interest seems to provides accurate results in this case, yet its applicability elsewhere depends on the terrain morphology, flight altitude, light and surface conditions. GNSS measurements covering the entire glacier are however labor intensive and it is recommended to acquire GNSS measurement outside the glacier area in relative flat areas which are easily identifiable, stable and will not experience surface elevation changes, e.g. center points of large boulders. These points can be used in subsequent UAV missions as virtual markers in the image processing if GNSS campaigns are not feasible.

The ortho-mosaic generated from the UAV imagery in combination with OBIA provides a suitable approach for the semi-automated mapping of the snow line and the terminus position. However, a manual inspection and digitization is needed to correct for debris covered parts of the glacier.

6. Acknowledgements

The authors thank Ånund Kvambekk, NVE, for field assistance and Bjarne Kjøllmoen, NVE, for dGNSS processing. This project has received funding from the European Research Council (ERC) under the European Union’s Horizon 2020 research and innovation program (grant agreement No 676819).

7. References

Agisoft LLC: Agisoft PhotoScan User Manual Professional Edition, Version 1.1, Agisoft, St. Petersburg, Russia., 2014.

Andreassen, L. M.: Comparing traditional mass balance measurements with long-term volume change extracted from topographical maps: a case study of Storbreen glacier in Jotunheimen, Norway, for the period 1940–1997, Geogr. Ann., 81A(4), 467–476, 1999.

The Cryosphere Discuss., doi:10.5194/tc-2016-292, 2017
Manuscript under review for journal The Cryosphere
Published: 5 January 2017

Andreassen, L. M., Elvehøy, H., Kjøllmoen, B. and Engeset, R. V.: Reanalysis of long-term series of glaciological and geodetic mass balance for 10 Norwegian glaciers, Cryosph., 10(2), 535–552, doi:10.5194/tc-10-535-2016, 2016.

Bader, H.: Sorge's law of densification of snow on high polar glaciers, J. Glaciol., 2(15), 319–323, 1954.

Bhardwaj, A., Sam, L., Martín-torres, F. J. and Kumar, R.: Remote Sensing of Environment UAVs as remote sensing platform in glaciology : Present applications and future prospects, Remote Sens. Environ., 175, 196–204, doi:10.1016/j.rse.2015.12.029, 2016.

Blaschke, T.: Object based image analysis for remote sensing, ISPRS J. Photogramm. Remote Sens., 65(1), 2–16, doi:10.1016/j.isprsjprs.2009.06.004, 2010.

Cogley, J. G.: Geodetic and direct mass-balance measurements : comparison and joint analysis, Ann. Glaciol., 50(50), 96–100, 2009.

Harder, P., Schirmer, M., Pomeroy, J. and Helgason, W.: Accuracy of Snow Depth Estimation in Mountain and Prairie Environments By an Unmanned Aerial Vehicle, Cryosph. Discuss., (February), 1–22, doi:10.5194/tc-2016-9, 2016.

Huss, M.: Density assumptions for converting geodetic glacier volume change to mass change, Cryosph., 7(4), 877–887, doi:DOI 10.5194/tc-7-877-2013, 2013.

Immerzeel, W. W., Kraaijenbrink, P. D. A., Shea, J. M., Shrestha, A. B., Pellicciotti, F., Bierkens, M. F. P. and de Jong, S. M.: High-resolution monitoring of Himalayan glacier dynamics using unmanned aerial vehicles, Remote Sens. Environ., 150, 93–103, doi:10.1016/j.rse.2014.04.025, 2014.

Jagt, B., Lucieer, A., Wallace, L., Turner, D. and Durand, M.: Snow Depth Retrieval with UAS Using Photogrammetric Techniques, Geosciences, 5(3), 264–285, doi:10.3390/geosciences5030264, 2015.

Kääb, a., Treichler, D., Nuth, C. and Berthier, E.: Brief Communication: Contending estimates of 2003 - 2008 glacier mass balance over the Pamir–Karakoram–Himalaya, Cryosph., 9(2), 557–564, doi:10.5194/tc-9-557-2015, 2015.

Kjøllmoen, B., Andreassen, L. M., Elvehøy, H., Jackson, M. and Giesen, R. H.: Glaciological investigations in Norway 2011-2015, Oslo., 2016.

Kraaijenbrink, P., Meijer, S. W., Shea, J. M., Jong, S. M. D. E. and Immerzeel, W. W.: Seasonal surface velocities of a Himalayan glacier derived by automated correlation of unmanned aerial vehicle imagery, Ann. Glaciol., 57, 103–113, 2016a.

Kraaijenbrink, P. D. A., Immerzeel, W. W., Pellicciotti, F. and Shea, J. M.: Distribution and characteristics of surface features on a debris-covered glacier, an object-based analysis, Remote Sens. Environ. (in Prep., 2016b.

Kraaijenbrink, P. D. A., Shea, J. M., Pellicciotti, F., De Jong, S. M. and Immerzeel, W. W.: Object-based analysis of unmanned aerial vehicle imagery to map and characterise surface features on a debris-covered glacier, Remote Sens. Environ., 186, 581–595, doi:10.1016/j.rse.2016.09.013, 2016c.

Lague, D., Brodu, N. and Leroux, J.: Accurate 3D comparison of complex topography with terrestrial laser scanner: Application to the Rangitikei canyon (N-Z), ISPRS J. Photogramm. Remote Sens., 82(February 2013), 10–26, doi:10.1016/j.isprsjprs.2013.04.009, 2013.

Liestøl, O.: Storbreen Glacier in Jotunheimen, Norway, Nor. Polarinst. Skr., 141, 5–62, 1967.

Lucieer, A., Jong, S. M. and Turner, D.: Mapping landslide displacements using Structure from Motion (SfM) and image correlation of multi-temporal UAV photography, Prog. Phys. Geogr., 38(1), 97–116, doi:10.1177/0309133313515293, 2013.

Magnússon, E., Belart, J. M. C., Pálsson, F., Ágústsson, H. and Crochet, P.: Geodetic mass balance record with rigorous uncertainty estimates deduced from aerial photographs and LiDAR data – case study from Drangajökull ice cap, NW-Iceland, Cryosph. Discuss., 9(5), 4733–4785, doi:10.5194/tcd-9-4733-2015, 2015.

De Michele, C., Avanzi, F., Passoni, D., Barzaghi, R., Pinto, L., Dosso, P., Ghezzi, A., Gianatti, R. and Vedova, G. Della: Using a fixed-wing UAS to map snow depth distribution: An evaluation at peak accumulation, Cryosphere, 10(2), 511–522, doi:10.5194/tc-10-511-2016, 2016.

Nolan, M., Larsen, C. and Sturm, M.: Mapping snow depth from manned aircraft on landscape scales at centimeter resolution using structure-from-motion photogrammetry, Cryosphere, 9(4), 1445–1463, doi:10.5194/tc-9-1445-2015, 2015.

Nuth, C. and Kääb, a.: Co-registration and bias corrections of satellite elevation data sets for quantifying glacier thickness change, Cryosph., 5(1), 271–290, doi:10.5194/tc-5-271-2011, 2011.

Pellicciotti, F., Stephan, C., Miles, E., Immerzeel, W. W. and Bolch, T.: Mass balance changes of the debris-covered glaciers in the Langtang Himal in Nepal between 1974 and 1999, J. Glaciol., 61, 373–386, 2015.

Rolstad, C., Haug, T. and Denby, B.: Spatially integrated geodetic glacier mass balance and its uncertainty based on geostatistical analysis: Application to the western Svartisen ice cap, Norway, J. Glaciol., 55(192), 666–680, doi:10.3189/002214309789470950, 2009.

Ryan, J. C., Hubbard, a. L., Box, J. E., Todd, J., Christoffersen, P., Carr, J. R., Holt, T. O. and Snooke, N.: UAV photogrammetry and structure from motion to assess calving dynamics at Store Glacier, a large outlet draining the Greenland ice sheet, Cryosph., 9(1), 1–11, doi:10.5194/tc-9-1-2015, 2015.

Saloranta, T. M.: Simulating snow maps for Norway: Description and statistical evaluation of the seNorge snow model, Cryosphere, 6(6), 1323–1337, doi:10.5194/tc-6-1323-2012, 2012.

Szelisky, R.: Computer Vision: Algorithms and Applications, edited by D. Gries and F.

The Cryosphere Discuss., doi:10.5194/tc-2016-292, 2017
Manuscript under review for journal The Cryosphere
Published: 5 January 2017

The Cryosphere Discussions
Open Access
EGU

Schneider, Springer-Verlag, London., 2011.

Trimble: eCognition Developer User Guide, Version 9.1.2, Trimble Documentation, Munich, Germany., 2015.

Vincent, C., Wagnon, P., Shea, J. M., Immerzeel, W. W., Kraaijenbrink, P. D. A., Shrestha, D., Soruco, A., Arnaud, Y., Brun, F., Berthier, E. and Sherpa, S.: Reduced melt on debris-covered glaciers: investigations from Changri Nup Glacier, Nepal, Cryosph. Discuss., 1–28, 2016.

Westoby, M. J., Brasington, J., Glasser, N. F., Hambrey, M. J. and Reynolds, J. M.: "Structure-from-Motion" photogrammetry: A low-cost, effective tool for geoscience applications, Geomorphology, 179, 300–314, doi:10.1016/j.geomorph.2012.08.021, 2012.

Westoby, M. J., Dunning, S. A., Woodward, J., Hein, a. S., Marrero, S. M., Winter, K. and Sugden, D. E.: Interannual surface evolution of an Antarctic blue-ice moraine using multi-temporal DEMs, Earth Surf. Dyn., 4, 515–529, doi:10.5194/esurf-4-515-2016, 2016.

Winsvold, S. H., Andreassen, L. M. and Kienholz, C.: Glacier area and length changes in Norway from repeat inventories, Cryosphere, 8(5), 1885–1903, doi:10.5194/tc-8-1885-2014, 2014.

Zemp, M., Thibert, E., Huss, M., Stumm, D., Denby, C. R., Nuth, C., Nussbaumer, S. U. and Moholdt, G.: The Cryosphere Reanalysing glacier mass balance measurement series, , 1227–1245, doi:10.5194/tc-7-1227-2013, 2013.

Tables

Table 1 Overview of the flight details

Flight	Date	Start time	End time	Duration	Images	Altitude (m)	Area (km^2)	Comments
1	09 Sep 15	10:09	10:27	0:18	168	359	1.50	-
2	09 Sep 15	11:03	11:24	0:21	210	251	1.99	-
3	09 Sep 15	12:02	12:08	0:06	70	238	0.86	Camera battery malfunction
4	09 Sep 15	12:49	12:56	0:07	76	230	0.64	Camera battery malfunction
5	10 Sep 15	10:19	10:35	0:16	160	318	1.28	Launched from terminus
6	10 Sep 15	11:10	11:29	0:19	231	245	1.23	Launched from terminus

Figures

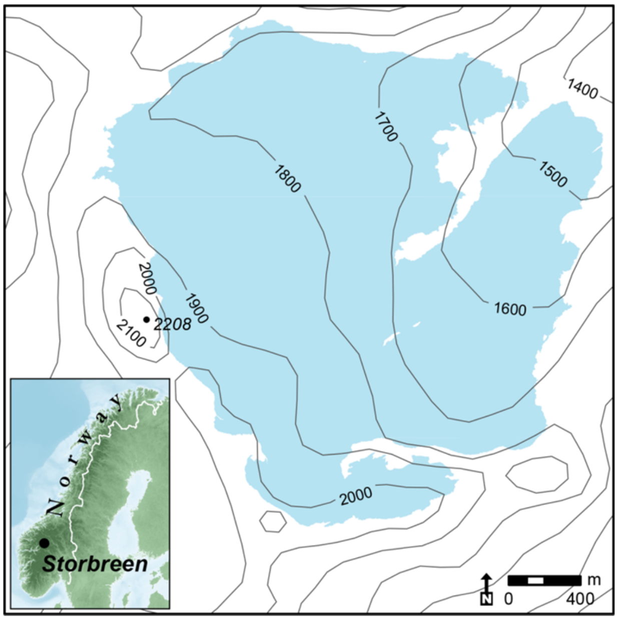

Figure 1 Location map of Storbreen in Norway. (source of contour lines: http://data.kartverket.no/download/content/n250-kartdata-utm33-hele-landet-fgdb) The glacier extent is from the 2009 survey.

The Cryosphere Discuss., doi:10.5194/tc-2016-292, 2017
Manuscript under review for journal The Cryosphere
Published: 5 January 2017

The Cryosphere
Discussions
Open Access

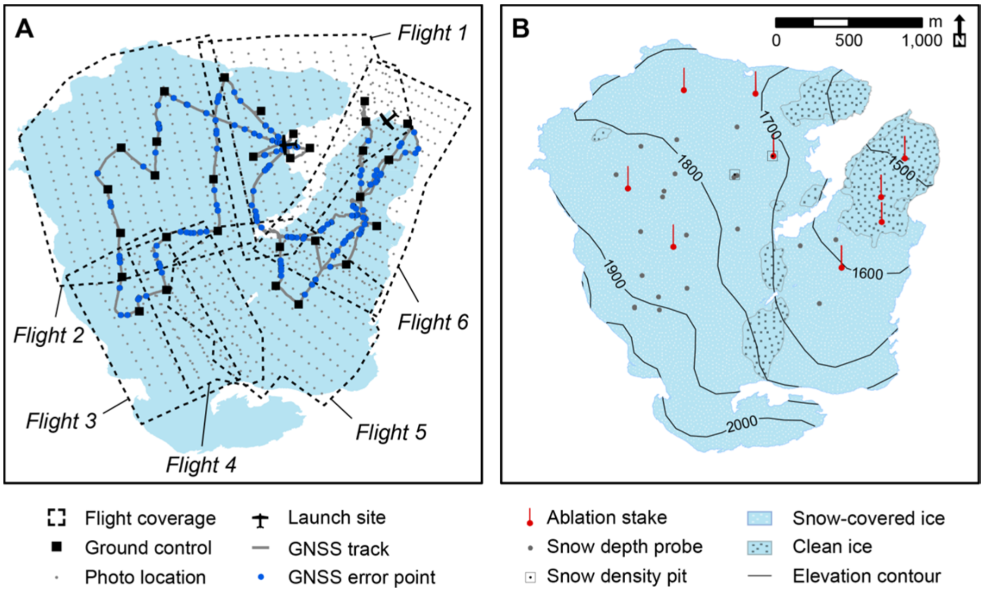

Figure 2 Overview of the flight tracks, GCPs, photo locations, GNSS points and launch site (panel A) and ablation stakes, snow depth probes and snow density pits (panel B)

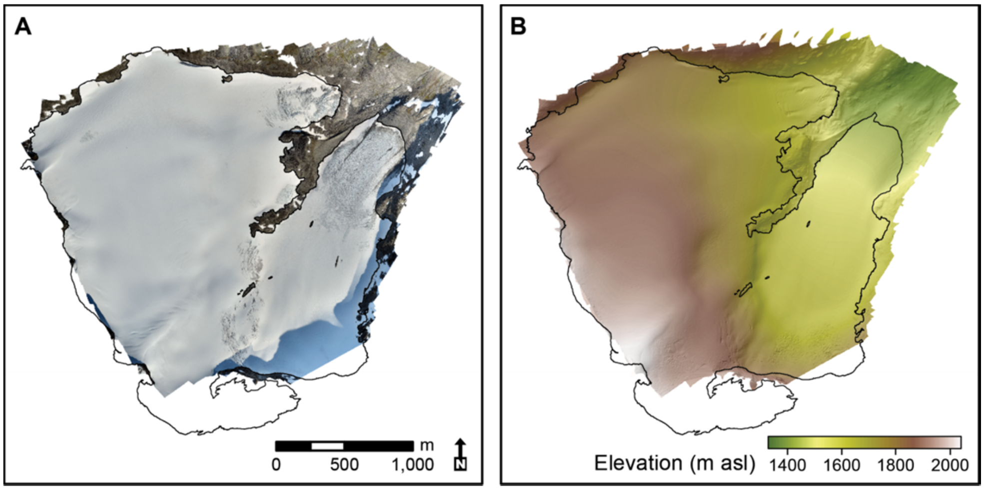

Figure 3 The ortho-mosaic and DEM of Storbreen from the 2015 UAV campaign at 0.25 m resolution

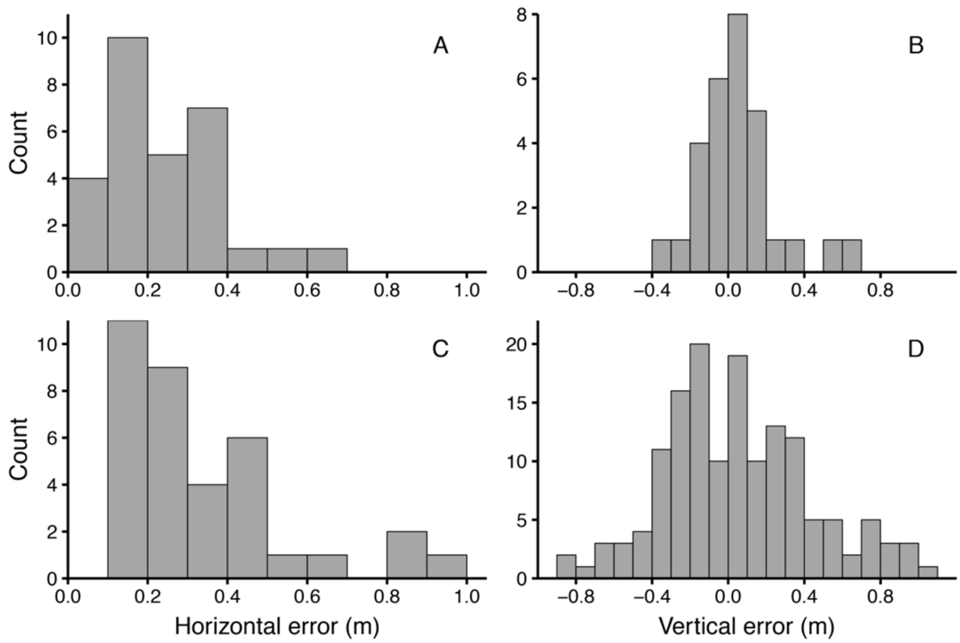

Figure 4 Errors between the SfM derived orthomosaic (horizontal) and elevation model (vertical), and the GNSS measurements of the 30 GCPs (a, b) and the independent points selected randomly from the DGPS track (c (n=41), d (n=150)). Random points were selected only from the parts of the GNSS track further than 50 meter from a GCP and where the rover was moving

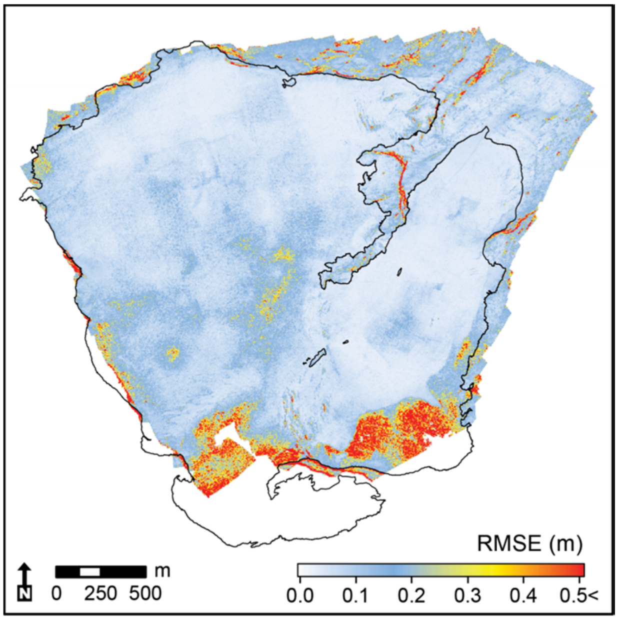

Figure 5 Spatial RMSE of the 2015 UAV DEM based on residual analysis of linear correlation of dense point cloud within 2 meter bins.

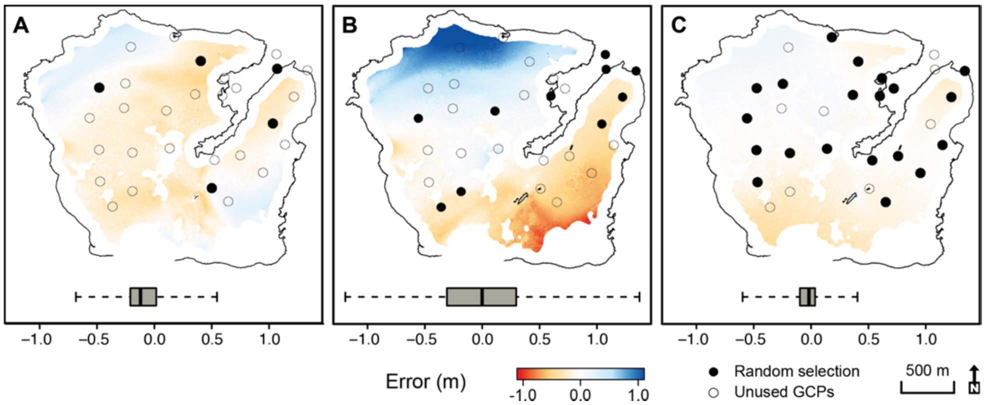

Figure 6 Impact of the number and distribution of markers used in the Agisoft processing. The black dots are markers used in the processing, whereas white dots are not used. All plots show elevation differences relative to case where all 30 markers were used. The boxplot shows the distribution of elevation differences for the three experiments (5 (panel A), 10 (panel B) and 20 (panel C markers respectively).

The Cryosphere Discuss., doi:10.5194/tc-2016-292, 2017
Manuscript under review for journal The Cryosphere
Published: 5 January 2017

The Cryosphere
Discussions
Open Access

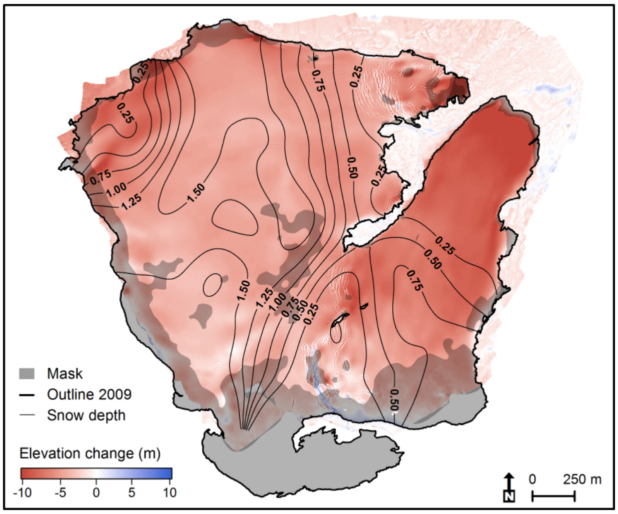

Figure 7 Elevation changes between 2009 LIDAR and 2015 UAV determined by cloud to cloud comparison in CloudCompare. The interpolated snow depth is shown as contour lines.

The Cryosphere Discuss., doi:10.5194/tc-2016-292, 2017
Manuscript under review for journal The Cryosphere
Published: 5 January 2017

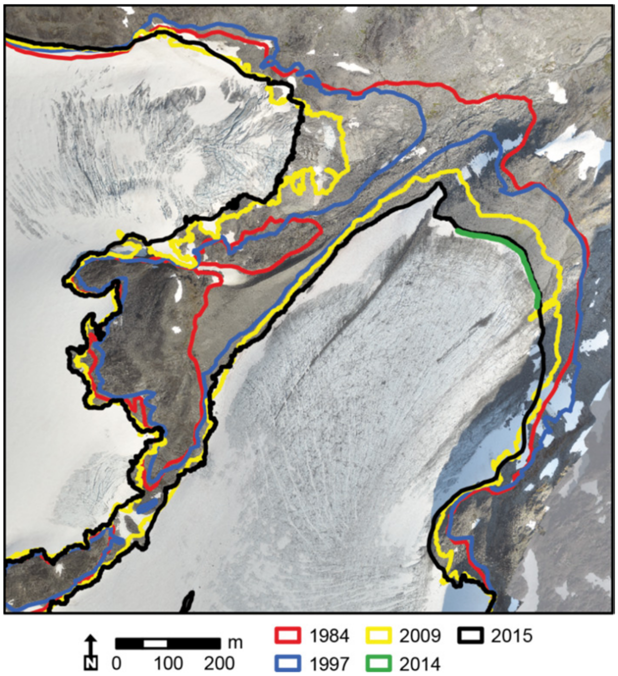

Figure 8 The retreat of the Storbreen glacier between 1984 and 2015 shown on the 2015 orthophoto. Outlines are from the glacier maps, except 2014, which is a GNSS survey of part of the southern terminus.